THE JOURNAL OF NAVIGATION (2011), **64**, S113–S126. © The Royal Institute of Navigation
doi:10.1017/S0373463311000324

Estimation and Mitigation of the Main Errors for Centimetre-level Compass RTK Solutions over Medium-Long Baselines

Hairong Guo[1], Haibo He[1], Jinlong Li[2] and Aibing Wang[1]

[1](*P.O. Box 5128, Beijing 100094, China*)
[2](*Institute of Surveying and Mapping of Information Engineering University, Zhengzhou, China*)
(Email: hairongguo@263.net)

Centimetre-level RTK solutions are mainly influenced by satellite orbit errors, ionospheric and tropospheric delays, and measurement noise (including multipath effects). Estimation and mitigation of the main errors for the CM-level Compass RTK solutions over medium-long baselines are investigated. Tests conducted for this research lead to the following conclusions:

1. For 100 km baselines, a 4 cm error in height component will be induced by a 10 m orbit error. For longer baselines, rapid precise ephemeris will be needed for CM-level accuracy RTK solutions.
2. The residual ionospheric delay error can be eliminated using the optimal triple-frequency ionosphere-free linear combination with the coefficients of 2·6087, −0·5175 and −1·0912 respectively for observations on f1, f2 and f3 frequencies. This combination is optimal in terms of its noise level, e.g., the noise is only amplified three times. It can be used for high accuracy RTK positioning.
3. The residual tropospheric delay can be resolved for the introduced relative zenith tropospheric delay (RZTD) parameters.

It is shown that the RTK solutions estimated from the least squares (LS) with the RZTD parameters are worse than that without these parameters. For instance, the errors in the height components are amplified approximately three times, which may be caused by the strong correlation between the introduced RZTD parameters and the height components. However, considering the fact that the residual zenith tropospheric delays vary slowly with time and the variation can be assumed to follow a random walk process, the RTK solutions can be improved using the Kalman filter and *a priori* information for the RZTD parameters.

KEY WORDS

1. Compass. 2. Medium-long baselines. 3. RTK.
4. Relative Zenith Tropospheric Delay (RZTD).

1. INTRODUCTION. Currently, GNSS precise positioning has been widely applied in both military and civilian fields. Due to the fact that the GPS data available from the current GNSS systems are only single or/and dual-frequency observations,

for precise real-time kinematic (RTK) positioning applications over medium-long baselines it has limitations in efficiency, coverage of its operation and positioning accuracy. For short baselines ($\leqslant$10 km), the typical on-the-fly RTK initialisation time with single-frequency receivers is about 15 minutes and that value is about three minutes with dual-frequency receivers. However for a medium-long baseline RTK, carrier phase ambiguities generally can hardly be successfully determined even using dual-frequency data. Hence the need for fast and efficient kinematic positioning over medium-long distances cannot be satisfied (Fan and Wang, 2007; Guo et al, 2010; He et al, 2010).

Compass, which is currently being built for China, will transmit three carrier signals for military and civilian uses. The availability of the multiple frequency signals will bring out a great advantage for fast precise relative positioning. For example, using the triple-frequency measurements from the Compass satellite system, instantaneous initialisation and CM-level accuracy RTK positioning will be possible for short baselines. And for medium-long baselines, carrier ambiguities can be more easily and successfully determined so that high accuracy RTK positioning results can be obtained without the need for resetting or moving the reference station. This means that the efficient and operational RTK coverage can be extended to a larger area without significant degradation of the positioning accuracy. The other benefit of using the triple-frequency Compass data is that the reliability of the positioning results will also be significantly improved and hence it will provide a more efficient technique for many areas of GNSS RTK applications such as marine surveying, aerial surveying, space surveying, boundary and reefs surveying (including boundary surveying, the joint surveying of the mainland and islands, and continental shelf and islands surveying) etc. Therefore, the implementation of high accuracy RTK positioning over medium-long baselines using the triple-frequency carrier phase observations from the Compass GPS system is a very important research topic for the second-generation GNSS applications.

Research for high accuracy, triple-frequency Compass RTK positioning over medium-long baselines mainly includes the following three categories: 1) Real-time cycle slip detection and recovery for triple-frequency observations; 2) Fast ambiguity resolution for medium-long baselines; and 3) High accuracy RTK positioning for medium-long baselines. At present, researchers all over the world have conducted much work for the first two categories, however, little literature for 3) can be found (Fan and Wang, 2007; Feng, 2008; Feng and Li, 2008a,2008b; Feng and Rizos, 2009; Feng et al, 2007; Guo et al, 2010; Han and Rizos, 1999; Hatch, 2006; He et al, 2010; Li 2010; Li et al, 2011; Teunissen et al, 2002). In this paper, the main error sources for high accuracy RTK positioning over medium-long baselines will be analysed first, then in-depth studies over the methods for the estimation and mitigation of the main errors are carried out. Finally, the validation of the above methods will be presented using Compass simulation observations (5GEO + 5 IGSO + 2 MEO).

2. MAIN ERRORS FOR CENTIMETRE-LEVEL COMPASS RTK POSITIONING OVER MEDIUM-LONG BASELINES.

2.1. *Satellite orbit errors.* The satellite orbit error is the difference between the satellite position predicted in satellite ephemeris and the true position of the satellite. Most of the satellite orbit error can be mitigated by differential techniques. However,

https://doi.org/10.1017/S0373463311000324 Published online by Cambridge University Press

Table 1. Errors in baselines of different lengths induced by the satellite orbit error of 10 m.

Baseline length (km)	Baseline error (mm)
10	3
50	15
100	30
500	150
1000	300

the residual orbit error in the differenced observables for a long baseline may still not be negligible so its effects on the positioning accuracy may still be significant.

Let dx be the error in a baseline and it is induced by the satellite orbit error d_{orb}, and let the length of the baseline be l, then the following equation can be used to calculate dx, i.e.

$$dx(m) \approx \frac{l}{d} \cdot d_{orb}(m) \approx \frac{l(km)}{35{,}786(km)} \cdot d_{orb}(m) \tag{1}$$

where d is the orbit altitude of Compass GEO satellites and IGSO satellites and $d \approx 35{,}786$ km.

According to equation (1), the errors induced by the 10 m satellite orbit error in baselines of various lengths are listed in Table 1. From this table, we can see: first, that the error in the baselines of lengths under 10 km is less than 3 mm, so it can be ignored for centimetre-level RTK positioning; and second, that the error values are about 3 cm, 15 cm, and 30 cm corresponding to the baselines with lengths of 100 km, 500 km and 1000 km respectively. This indicates that the effects of the satellite orbit error on long baselines (e.g., >100 km) are significant, thus it needs to be mitigated for high accuracy GNSS positioning.

2.2. *Ionospheric delay error*. The ionosphere is the part of the atmosphere that is in the layer of 50–1000 km above the surface of the earth. The ionosphere is partially ionized because of solar radiation. It is the layer with a high density of free electrons. When GPS signals transmit through the ionosphere, they will be refracted, and the phase velocity will be increased whilst the group velocity of the pseudo-range (group velocity) will be decreased.

The ionospheric effects on GNSS observables can be greatly reduced using differential techniques. For short baselines (e.g., <10 km), the residual ionospheric error is very small and will not affect the baseline's ambiguity resolution. However, for long baselines, the residual ionospheric error may still be significant and that will cause difficulty to quickly resolve the baseline's ambiguity.

On the other hand, even though the ambiguity has been successfully resolved for short baselines of several kilometres, the effects of the residual ionospheric delay errors cannot be always neglected, for example, in the application for the monitoring of deformation networks, as the scale factor of the baseline will be affected. The magnitude of the effects of the residual ionospheric delay errors are dependent upon the linear combinations used and the elevation angle $E_{\min}$. Generally, the ionospheric delay error in GNSS observables is proportional to the total electron content (TEC) in the signal propagation path. TECU is often used as the unit of TEC, and one

https://doi.org/10.1017/S0373463311000324 Published online by Cambridge University Press

TECU = 1016 electron/m^2. For the observables on the Compass B1 frequency, when the elevation cut-off angle of 15° is used, the effect of the residual ionospheric error of 10 TECU is about 1·0 ppm (i.e., 1·0 mm/km). Therefore, for medium-long baselines, the residual ionospheric delay errors should be taken into account, which is not only for ambiguity resolution but also for precise kinematic positioning.

2.3. *Tropospheric delay error*. The tropospheric delay generally refers to the refraction of electromagnetic waves caused by the neutral atmospheric part. The neutral atmosphere is the lower part of the atmosphere and it mainly includes the troposphere and stratosphere, which is approximately from the ground surface of the earth up to 50 km. Due to the fact that about 80% of the refraction is caused by the troposphere, the delay caused by the whole neutral atmosphere is usually called the troposphere delay.

The tropospheric delay consists of the dry and wet components. About 80 to 90% of the tropospheric delay is caused by the dry component (i.e., the dry gas) in the atmosphere. The remaining 10 to 20% of the tropospheric delay is caused by water vapour, i.e., the wet component. The typical value of the dry delay in the zenith direction is 2·3 m, and of the wet delay is about 1 to 80 cm. The tropospheric delay depends on many factors such as the climate, air pressure, temperature, humidity and elevation of the satellite. For low elevation satellites, the total tropospheric delay can reach 30 m.

The troposphere is a non-dispersive medium for GNSS signals, hence the tropospheric delay cannot be calculated from dual-frequency GNSS observations. For short baselines with small height differences, if differential techniques are used, the effects of the tropospheric delay errors can be greatly reduced. However, for long baselines or baselines with large height differences, even the same differential techniques are used, the residual tropospheric delay errors may not be negligible and so they may significantly affect both ambiguity resolution and baseline solutions. For aviation users, when a baseline's height difference is more than 6000 m, the error in the height difference induced by the residual tropospheric delay errors can reach 5 m.

According to the analysis of the residual tropospheric delay effects on baseline solutions, the residual tropospheric delay can be roughly divided into two kinds: relative and absolute tropospheric delays.

The relative tropospheric delay is the difference between the tropospheric delays at the rover station and the base station. Its effect on the baseline's height component is particularly remarkable. The error in the height component caused by the relative tropospheric delay can be calculated by:

$$\Delta h = \frac{\Delta d_{trop}}{\sin E_{\min}} \tag{2}$$

where Δd_{trop} is the relative tropospheric delay and $E_{\min}$ is the satellite elevation angle. When $E_{\min} = 20°$, 1 mm Δd_{trop} will lead to a 3 mm error in the height component.

The absolute tropospheric delay is a common part of the tropospheric effects in both the rover station and the base stations. The scale factor of the baseline affected by the absolute tropospheric delay can be calculated by:

$$\frac{\Delta l}{l} = \frac{d_{trop}}{R_e \sin E_{\min}} \tag{3}$$

https://doi.org/10.1017/S0373463311000324 Published online by Cambridge University Press

where d_{trop} is the absolute tropospheric delay, l and Δl are the baseline length and the difference of the baseline caused by d_{trop} respectively, R_e is the Earth radius. When $E_{\min} = 20°$, a 2 m of d_{trop} will lead to about 1 ppm scale error.

Similar to the orbit errors, the residual tropospheric delay errors will also affect baseline solutions and geometry-based ambiguity resolutions. However, considering that the residual tropospheric delay errors have the same values in the triple-frequency observations of a satellite, the ambiguity resolution based on the geometry-free mode are not influenced.

2.4. *Multi-path effects*. The GNSS receiver receives not only the signals directly from satellites but also the signals reflected from the surrounding buildings or objects. The reflected signals interfere with the direct ones and their effects are called multi-path effects. The multi-path effect is one of the main errors affecting high accuracy positioning especially for short baselines. Multi-path effects on pseudorange measurements can reach up to 1/2 of the code length whereas on carrier phase measurements are very small, e.g., their maximum value is about 1/4 of the carrier wavelength.

In the static measurement, multi-path effects show a periodic sinusoidal variation with the change of the satellite geometry. The part for the variation of the long-period can be estimated. The part for the variation of the short-period can be absorbed by the residuals and the effects can be eliminated using the time averaging method.

In the kinematic positioning, multi-path effects can be treated as random errors due to the changing of the measurement environment. However, for a low-speed moving receiver, multi-path effects tend to vary periodically when its surrounding objects/environments do not change much.

Multi-path effects are related to the direction of the satellite signal, the reflection coefficient and the range from a reflector. They are difficult to model due to the complex measurement environments. They cannot be mitigated by differencing methods. Generally, careful selection of sites is recommended to avoid potential multi-path effects, e.g., making the antenna away from reflectors, using choke ring antennas, improving the code and phase tracking loop and so on. In the data processing, multi-path effects are usually treated as random errors thus they can be combined with the observation noise to make the two error terms become one.

2.5. *Measurement noise*. The measurement noise is usually considered to be white noise, and the measurement noise among observations of different satellites is uncorrelated. The measurement noise is associated with the code correlation mode, receiver dynamic status and satellite elevation. The pseudorange noise is about 0·3 m (B3) or 0·6 m (B1/B2) for Compass, the phase noise is generally 1% percent of its wavelength. For different types of receivers and signal noise ratios, the phase noise varies between 0·1% $\sim$ 3% of the wavelength.

3. METHODS FOR ESTIMATION AND MITIGATION OF THE MAIN ERRORS.

3.1. *Strategy for mitigating orbit error effects*. As mentioned before, orbit errors will have effects on the geometry-based ambiguity resolution and baseline solutions. For medium-long baselines, the effects of orbit errors on baseline solutions are proportional to baseline lengths. For a baseline of 100 km, the baseline error induced by a 10 m orbit error (Compass satellites) is about 3 cm. For longer baselines, the orbits provided by the broadcast ephemeris may significantly affect the accuracy of RTK positioning. Hence, the precise ephemeris for Compass should be studied and

https://doi.org/10.1017/S0373463311000324 Published online by Cambridge University Press

used to mitigate the effects of orbit errors for RTK positioning applications over medium-long baselines.

3.2. *Optimal ionosphere-free combinations of triple-frequency observations of Compass*. The ionospheric delay error is one of the most severe errors in GNSS observations and this error will significantly affect baseline solutions even using differenced observations for medium-long baselines. However, most part of the ionospheric delay error can be eliminated from a proper linear combination, e.g., the so-called ionosphere-free combinations of different frequency observations. This is because the ionosphere is a dispersive medium thus its delay error depends on the signal frequency.

An ionosphere-free linear combination of triple-frequency observations can be expressed as:

$$\Phi_M = \alpha \cdot \nabla\Delta\Phi_1 + \beta \cdot \nabla\Delta\Phi_2 + \gamma \cdot \nabla\Delta\Phi_3 \tag{4}$$

$$\Phi_M = (\alpha+\beta+\gamma)\nabla\Delta\rho - \left(\frac{\alpha}{f_1^2}+\frac{\beta}{f_2^2}+\frac{\gamma}{f_3^2}\right)\nabla\Delta K_1 + (\alpha \cdot \nabla\Delta\varepsilon_{\Phi_1} + \beta \cdot \nabla\Delta\varepsilon_{\Phi_2} + \gamma \cdot \nabla\Delta\varepsilon_{\Phi_3}) \tag{5}$$

Equation (5) can be rewritten in the following form:

$$\Phi_M = (\alpha+\beta+\gamma)\nabla\Delta\rho - \left(\frac{\alpha}{f_1^2}+\frac{\beta}{f_2^2}+\frac{\gamma}{f_3^2}\right)\nabla\Delta K_1 + \left(\alpha \cdot \frac{C}{f_1} + \beta \cdot \frac{C}{f_2} + \gamma \cdot \frac{C}{f_3}\right)\sigma_{\nabla\Delta\varphi} \tag{6}$$

where α, β, γ should satisfy the following conditions:

$$\alpha+\beta+\gamma = 1 \tag{7}$$

$$\frac{\alpha}{f_1^2}+\frac{\beta}{f_2^2}+\frac{\gamma}{f_3^2} = \frac{A}{f_1^2} \tag{8}$$

$$\alpha^2 + C_1 \cdot \beta^2 + C_2 \cdot \gamma^2 = \min \tag{9}$$

where, $\nabla\Delta K_1/f_1^2$ is double-difference ionospheric delay for the observations on the frequency B_1; C is the velocity of the light; $\sigma_{\nabla\Delta\varphi}$ is phase error (including measurement noise and multipath) in units of cycles for all the three frequencies; A is the ionospheric coefficient of the combination and it is generally assumed to be 0 for ionosphere-free combinations; C_1 and C_2 are the noise coefficient ratios of $\nabla\Delta\Phi_2$ and $\nabla\Delta\Phi_3$ to $\nabla\Delta\Phi_1$ respectively, and $C_1 = (f_1/f_2) \cdot (f_1/f_2)$, $C_2 = (f_1/f_3) \cdot (f_1/f_3)$.

From Equation (7), one can obtain:

$$\gamma = 1 - \alpha - \beta$$

Substitute this equation to Equation (8):

$$\alpha f_2^2 f_3^2 + \beta f_1^2 f_3^2 + (1-\alpha-\beta) f_1^2 f_2^2 = A f_2^2 f_3^2$$

$$\beta = \frac{f_2^2}{f_1^2} \cdot \frac{(f_1^2 - A f_3^2)}{f_2^2 - f_3^2} - \alpha \frac{f_2^2}{f_1^2} \cdot \frac{f_1^2 - f_3^2}{f_2^2 - f_3^2}$$

Let $\beta = F_a - \alpha F_b$ and

$$F_a = \frac{f_2^2}{f_1^2} \cdot \frac{(f_1^2 - A f_3^2)}{f_2^2 - f_3^2}$$

https://doi.org/10.1017/S0373463311000324 Published online by Cambridge University Press

$$F_b = \frac{f_2^2(f_1^2 - f_3^2)}{f_1^2(f_2^2 - f_3^2)}$$

Then Equation (9) has the form:

$$\alpha^2 + C_1 \cdot (F_a - \alpha F_b)^2 + C_2 \cdot (1 - \alpha - F_a + \alpha F_b)^2 = \min$$

Let $v = [C_1 F_a^2 + C_2(1 - F_a)^2] - 2a[C_1 F_a F_b + C_2(1 - F_a)(1 - F_b)] + \alpha^2[1 + C_1 F_b^2 + C_2(1 - F_b)^2]$.

Assuming that the derivative of v is equal to 0, then one can obtain:

$$\alpha = \frac{C_1 F_a F_b + C_2(1 - F_a)(1 - F_b)}{1 + C_1 F_b^2 + C_2(1 - F_b)^2}$$

Combined with the aforementioned two formulae:

$$\beta = F_a - \alpha F_b$$

$$\gamma = 1 - \alpha - \beta$$

Assuming $A = 0$, $C_1 = (f_1/f_2) \cdot (f_1/f_2)$ and $C_2 = (f_1/f_3) \cdot (f_1/f_3)$, that is to say, the phase error in units of cycles for all the three frequencies is $\sigma_{\nabla\Delta\varphi}$, then the derived coefficients of the optimal ionosphere-free combination of the triple-frequency observations are:

$$\alpha = 2{\cdot}6087$$

$$\beta = -0{\cdot}5175$$

$$\gamma = -1{\cdot}0912$$

From these values, one can also obtain:

$$\sqrt{\alpha^2 + \beta^2 + \gamma^2} = 3{\cdot}0335$$

where the three frequencies of the Compass system are B1 = 1561·098 MHz, B2 = 1207·14 MHz and B3 = 1268·52 MHz respectively.

Then the standard deviation of Φ_M can be expressed as

$$\sigma_{[\Phi_M]} = 3{\cdot}0335 \cdot \lambda_1 \cdot \sigma_{\nabla\Delta\varphi} = 0{\cdot}0291\, m \tag{10}$$

where $\sigma_{\nabla\Delta\varphi} = 5\%$.

The noise coefficients and noise levels of dual-frequency and triple-frequency ionosphere-free combinations are summarized in Table 2, respectively. Table 2 shows that the noise coefficients of triple-frequency combinations are slightly better than that of dual-frequency combinations. Considering that the ionosphere-free combination is mainly used for precise positioning, then it is concluded that the triple-frequency combinations cannot be used for largely improving positioning accuracy. But triple-frequency observations will be used for determining carrier ambiguities more easily and successfully. For short baselines, instantaneous ambiguity initialization is feasible. And for medium-long baselines, ambiguities can be determined with the geometry-free method (Fan and Wang, 2007; Feng, 2008; Feng and Li, 2008a, 2008b; Feng and Rizos, 2009; Feng et al, 2007; Guo et al, 2010; Han and Rizos, 1999; Hatch, 2006; Li et al, 2011; Teunissen and Joosten, 2002; Teunissen et al, 2002).

3.3. *RZTD parameter estimation*. The tropospheric delay is one of the key limiting factors for the performance of high accuracy RTK positioning over medium-long

https://doi.org/10.1017/S0373463311000324 Published online by Cambridge University Press

Table 2. Ionosphere-free combinations.

Combination coefficients			Coefficients of combination noise	Combination noise (Metre)
α	β	γ		
$\frac{f_1^2}{f_1^2-f_2^2}$	$-\frac{f_2^2}{f_1^2-f_2^2}$	0	3·1440	0·0302
$\frac{f_1^2}{f_1^2-f_3^2}$	0	$-\frac{f_3^2}{f_1^2-f_3^2}$	3·7930	0·0364
2·6087	−0·5175	−1·0912	3·0335	0·0291

Note. The noise level of the above combinations is calculated under the assumption of $\sigma_{\nabla\Delta\varphi} = 5\%$.

baselines. In order to reduce the effect of the tropospheric delay, some scholars have proposed the introduction of RZTD parameters for the cases of baselines with either medium-long lengths or large height-difference. However, once the RZTD parameter is introduced along with coordinate parameters in the observation equation, the coefficient matrix of the normal equation of the Least Squares (LS) may be in an ill condition due to the strong correlation between the RTZD parameter and the height component. In this case, the parameter solution is not stable since a small error in the observation may cause a large error in the LS estimates.

Once the ambiguities of the baseline have been successfully resolved and cycle slips, if any, have been repaired, the centimetre-level accuracy RTK solutions over the medium-long baselines can be obtained using the Kalman filter. The LS can be used to estimate the coordinate and RZTD parameters for the current epoch if the prior information for the unknown parameters is not considered. The Kalman filter can also be used to acquire the estimates of the unknown parameters and their covariance if the prior information is considered. And the random walk model for residual tropospheric delay error should also be taken into account in the Kalman filter. However, one of the key issues in using the Kalman filter is how to determine the process noise and initial variances of the unknown parameters (Yang et al, 2010).

4. CALCULATION AND ANALYSIS.

In order to verify the effects of the main errors on precise RTK positioning over medium-long baselines, Compass observations need to be simulated first.

4.1. *Data Simulation*.

Due to the fact that, for precise positioning, the double differencing technique is commonly used so that the clock errors of the satellite and the receiver can be cancelled out, and the effects of the satellite orbit error, the ionospheric delay and the tropospheric delay can also be largely eliminated. In the simulation for the zero-difference Compass observations, the satellite orbit error, the ionospheric and the tropospheric delays, and the measurement noise (including multipath effects) should be taken into account. The magnitudes of these errors and the models used for the generation of some of these errors for Compass (5GEO + 5 IGSO + 2 MEO) are as follows:

- Satellite orbit error: 10 m;
- Ionospheric model: broadcast ionospheric model i.e., Kobuchar model;

https://doi.org/10.1017/S0373463311000324 Published online by Cambridge University Press

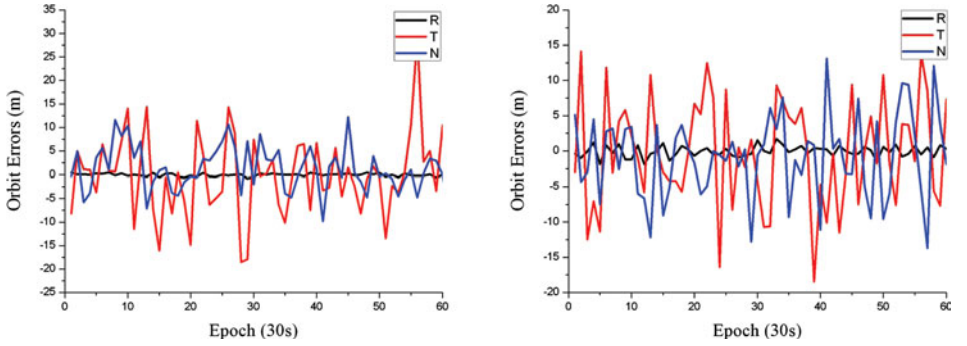

Figure 1. Simulated orbit errors for the COMPASS GEO (Left) and for the COMPASS IGSO/MEO (Right) satellites.

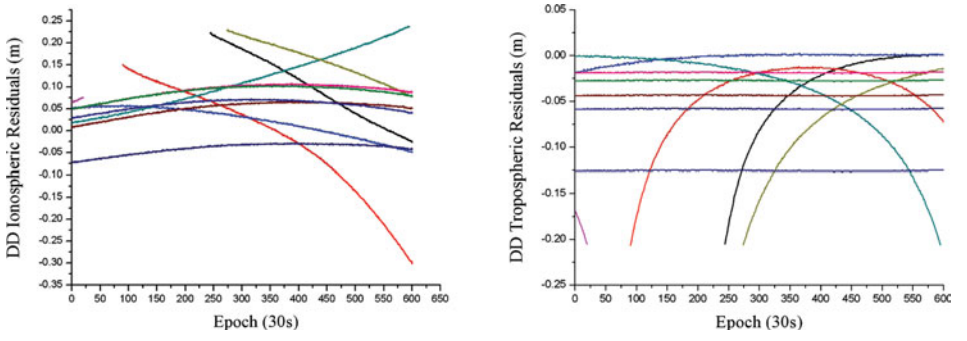

Figure 2. Simulated double-difference ionospheric (left) and tropospheric residuals for COMPASS (100 km baseline).

- Single-difference zenith ionospheric residuals for the B1 frequency: 0·5 ppm
- Tropospheric models: the SBAS tropospheric correction model
- Single-difference zenith tropospheric residual: 0·5 ppm

Multipath and receiver noise (zero-difference, 1σ):

- Pseudorange: B1: 0·6 m, B2: 0·6 m, B3: 0·3 m
- Carrier phase: 1% cycle

Based on these error levels and models, the zero-difference pseudorange and carrier phase observations for the Compass three frequencies B1, B2, and B3 were simulated. The data session is 24 hours, the sampling rate is 30 seconds, the elevation cut-off angle was set to 10 degrees, the baseline lengths are 50 km and 100 km (selected in the Beijing area) respectively, and the ambiguity was set to 0 for each frequency.

The simulated double-difference ionospheric and tropospheric residuals, pseudorange and carrier phase observations are shown in Figures 1–3.

4.2. *Analysis of the effects of orbit errors.* Over medium-long baselines (50 km and 100 km), the RTK positioning errors caused by a 10 m orbit error are shown in Figure 4. It can be seen that the positioning errors of the 100 km baseline are much

https://doi.org/10.1017/S0373463311000324 Published online by Cambridge University Press

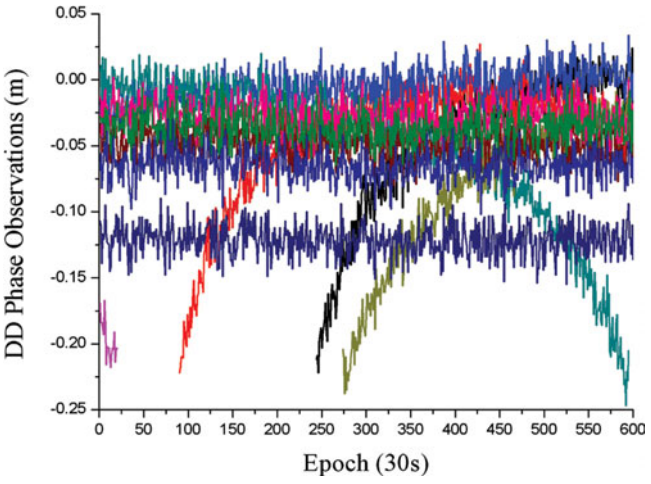

Figure 3. Simulated double-difference phase observations for COMPASS (the geometry distance and ionospheric delay are not included).

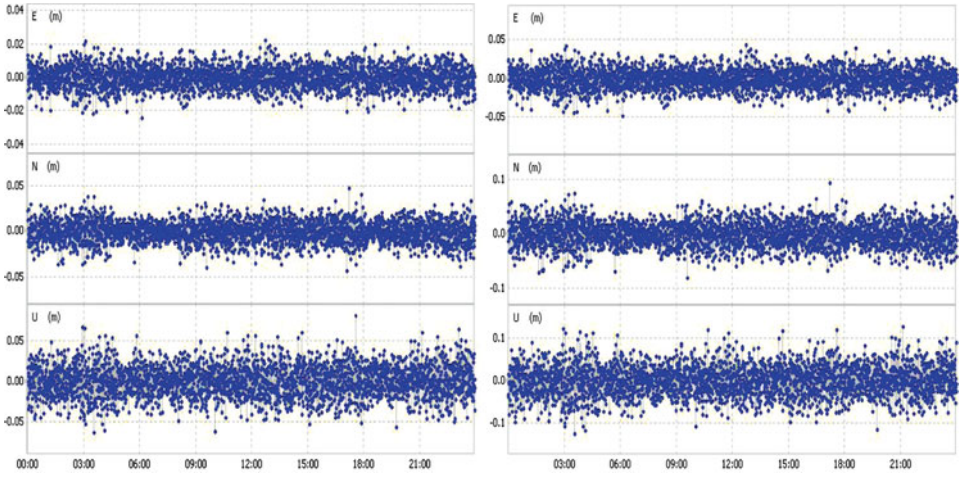

Figure 4. Positioning errors induced by a 10 m satellite orbit error of COMPASS satellites with 50 km baseline (left) and 100 km baseline (right).

larger than that of the 50 km baseline. This further verifies that the magnitude of the orbit error's effect on the accuracy of the RTK positioning is proportional to the baseline length. The RTK RMS errors in the three coordinate components E-W, N-S, U-D caused by the 10 m orbit error are 1·3 cm, 2·2 cm and 3·6 cm respectively over the 100 km baseline.

4.3. *LS estimation with RZTD parameters.* In order to verify whether it is reasonable to introduce the RZTD parameter in the LS estimation, the following two schemes were adopted to estimate the RTK positioning parameters.

https://doi.org/10.1017/S0373463311000324 Published online by Cambridge University Press

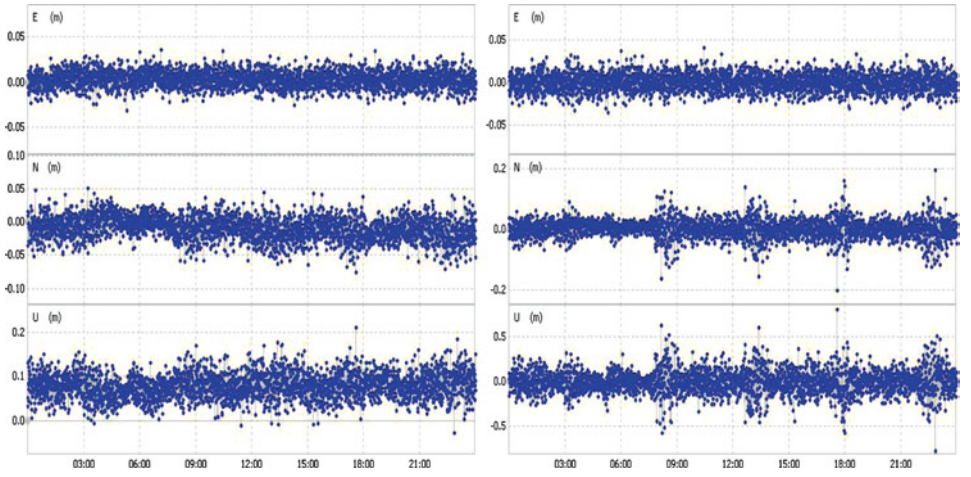

Figure 5. Positioning errors estimated from Scheme 1 (left) and Scheme 2 (right) with 50 km baseline.

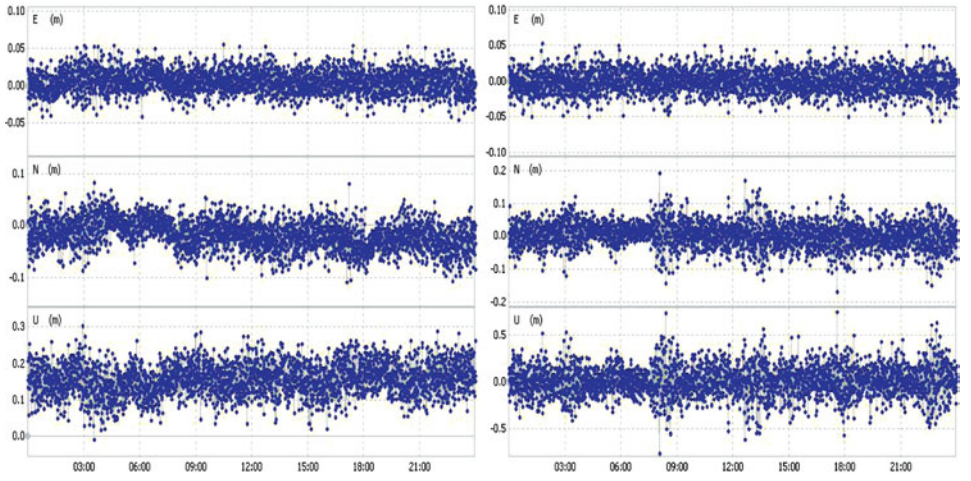

Figure 6. Positioning errors estimated from Scheme 1 (left) and Scheme 2 (right) with 100 km baseline.

Scheme 1: only the coordinate parameters (E/N/U) are estimated.
Scheme 2: the coordinate parameters (E/N/U) plus the RZTD parameter are estimated.

It is assumed that the baseline's ambiguities have been resolved successfully and the optimal triple-frequency ionosphere-free combination is used when estimating the positioning parameters based on the two schemes. The results are shown in Figures 5–7 and Table 3.

https://doi.org/10.1017/S0373463311000324 Published online by Cambridge University Press

Table 3. Comparison of positioning errors (cm) from the two schemes.

	Scheme 1 (without RZTD parameter)	
	50 km AVE/STD/RMS	100 km AVE/STD/RMS
E-W	0·4/0·9/1·0	0·7/1·5/1·6
N-S	0·9/1·8/2·0	1·7/2·7/3·2
U-D	***7·9***/2·9/8·4	***15·7***/4·3/16·3
RZTD	///	///
	Scheme 2 (with RZTD parameter)	
	50 km AVE/STD/RMS	100 km AVE/STD/RMS
E-W	0·0/1·0/1·0	0·0/1·6/1·6
N-S	0·3/3·1/3·1	0·6/3·8/3·9
U-D	0·4/***13·0/13·0***	1·0/***16·0/16·0***
RZTD	2·3/3·4/	4·5/4·1/

Note. RMS is calculated from the difference between the estimates and the known coordinates.

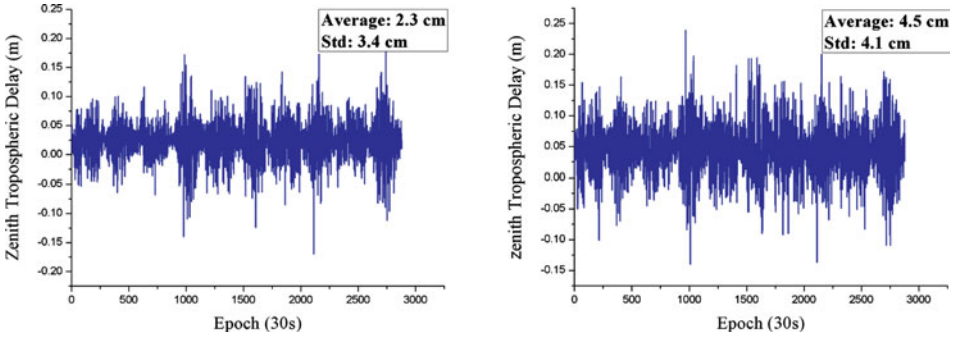

Figure 7. Tropospheric delay parameter estimated from Scheme 2 with 50 km baseline (left) and 100 km baseline (right).

From these results, we can see that, without introducing the RZTD parameter (Scheme 1), large means are in the height estimates (e.g., 7·9 cm and 15·7 cm are for the 50 km and 100 km baselines respectively). The reason is that the residual tropospheric delay error in a medium-long baseline's observation equation is large, and the large error is absorbed by the height estimate if it is not introduced and resolved as an unknown parameter. Although the mean values of the positioning errors estimated from Scheme 2 (with RZTD) are relatively small, the variances and RMS of the height components are all up to more than a dozen centimetres (e.g., 13·0 cm and 16·0 cm are for the 50 km and 100 km baselines respectively) and the reliability of the positioning solutions is very poor. From these results, the strong correlation between the RZTD and the height component estimates is further verified thus it should be considered in the RTK parameter estimation.

https://doi.org/10.1017/S0373463311000324 Published online by Cambridge University Press

5. CONCLUSION. The performance of RTK positioning over medium-long baselines is mainly affected by the orbit error, the ionospheric delay and the tropospheric delay. The test results in this paper show that:

1. A rapid precise ephemeris is needed for the centimetre-level RTK positioning for baselines of several hundred kilometres and longer.
2. The residual (first-order) ionospheric delay errors can be eliminated using the optimal triple-frequency ionosphere-free linear combination (with the coeficents of 2·6087, −0·5175, −1·0912 for the three frequencies of Compass respectively). The noise of this combination is only magnified 3 times. This combination can be used for high accuracy RTK positioning.
3. The results show that the RTK solutions from Scheme 2 where the RZTD parameter is estimated, are even worse than those from Scheme 1, where the RZTD parameter is not estimated. For instance, the height component error is approximately magnified 3 times, which is likely caused by the strong correlation between the introduced RZTD parameter and the height component. Considering that the residual zenith troposphere delay changes slowly in a short time and its variation appears to follow the random walk process, the RTK solutions can be improved with the Kalman filter.

ACKNOWLEDGEMENTS

The project is sponsored by Natural Science Foundations of China (41020144004).

REFERENCES

Fan, J. J. and Wang, F. X. (2007). A Method for GNSS Three Frequency Ambiguity Resolution Based on Short Baseline. *Acta Geodaetica et Cartographica Sinica*, **36**(1), 43–49 (in Chinese).

Feng, Y. M. (2008). GNSS Three Carrier Ambiguity Resolution using Ionosphere-reduced Virtual Signals. *Journal of Geodesy*, **82**(12), 847–862.

Feng, Y. M. and Li, B. F. (2008a). A Benefit of Multiple Carrier GNSS Signals: Regional Scale Network-based RTK with Doubled Inter-station Distances. *Journal of Spatial Sciences*, **53**(2), 135–147.

Feng, Y. M. and Li, B. F. (2008b). Three Carrier Ambiguity Resolutions: Generalized Problems, Models, Methods and Performance Analysis using Semi-generated Triple Frequency GPS Data. *Proceedings of ION GNSS 2008*, 2831–2840.

Feng, Y. M. and Rizos, C. (2009). Network-based Geometry-Free Three Carrier Ambiguity Resolution and Phase Bias Calibration. *GPS Solutions*, **13**(1), 43–56.

Feng, Y. M., Rizos, C. and Higgins, M. (2007). Multiple Carrier Ambiguity Resolution and Performance Benefits for RTK and PPP Positioning Services in Regional Areas. *Proceedings of ION GNSS 2007*, 668–678.

Guo, H. R., He, H. B. and Wang, A. B. (2010). The Method of Real-time GNSS Ambiguity Resolution for Short Baselines. *China Satellite Navigation Conference 2010*, 388. (in Chinese).

Han, S. W. and Rizos, C. (1999). The Impact of Two Additional Civilian GPS Frequencies on Ambiguity Resolutions Strategies. *Proceedings of ION ATM 1999*, 315–321.

Hatch, R. (2006). A New Three-frequency, Geometry-free Technique for Ambiguity Resolution. *Proceedings of ION GNSS 2006*, 309–316.

He, H. B., Guo, H. R. and Wang, A. B. (2010). Cycle Slip Recovery Method for Long-range Dual-frequency GPS Kinematic Surveying. *Journal of Geomatics Science and Technology*, **27**(6), 396–398 (in Chinese).

Li, B. F. (2010). Theory and Method for Parameter and Variance-covariance Component Estimation in Mixed Integer Linear GPS Model. Tongji University. (in Chinese).

Li, J. R., Yang, Y. X., Xu, J. Y., He, H. B. and Guo, H. R. (2011). Real-time Cycle-Slip Detection and Repair Based Code/Phase Combination for Triple-Frequency GNSS Undifferenced Observation Data. *Acta Geodaetica et Cartographica Sinica*, in Press (in Chinese).

Teunissen, P., Joosten, P. and Tiberius, C. (2002). A Comparison of TCAR, CIR and LAMBDA GNSS Ambiguity Resolution. *Proceedings of ION GPS 2002*, 2799–2808.

Yang, Y. X., Gao, W. G. and Zhang, X. (2010). Robust Kalman Filtering with Constraints: A Case Study for Integrated Navigation. *Journal of Geodesy*, 2010(**84**), 373–381.